Eur. Phys. J. B **4**, 65–74 (1998)

**THE EUROPEAN PHYSICAL JOURNAL B**



# A dynamic study of onion phases under shear flow: size changes

P. Panizza[a], A. Colin, C. Coulon, and D. Roux

Centre de Recherche Paul Pascal, avenue Dr Schweitzer, 33600 Pessac, France

Received: 14 November 1997 / Received in final form: 2 March 1998 / Accepted: 9 March 1998

**Abstract.** It has been shown that lyotropic lamellar phases under shear flow form structures corresponding to a close packed assembly of monodisperse multilamellar vesicles (onions). The size, which is fixed by the shear rate, can vary from a few microns to a tenth of a micron. In this study, we investigate for the first time the transient behaviour of size changes of onions under shear flow by means of small angle light scattering, direct microscopic observations, and conductivity measurements. We evidence two regimes: continuous and discontinuous. The nature of which (continuous or discontinuous) depends on the initial and final shear rate, and can be described by a dynamic phase diagram.

**PACS.** 83. Rheology – 64.60 Ht Dynamic critical phenomena – 61.30 Eb Experimental determinations of smectic, nematic, cholesteric, and other structures

## 1 Introduction

Classical fluid dynamics describes a fluid flow in terms of macroscopic variables such as velocities, pressure, temperature [1]. This description which has proved to be particularly well adapted to simple fluids, breaks down however for complex fluids (such as emulsions, polymers, colloidal suspensions and others...). The characteristic lengths of these fluids are indeed so large that the flow cannot be considered any longer as uniform at all scales. That is why a good analysis requires to take into account the coupling between the flow and the details of the fluid structure [2,3]. Recently much effort has been drawn to relate the complex rheological behaviour of such fluids to their microstructure [4–7]. These studies have obvious industrial and fundamental interests. In particular, one final perspective of such works is to relate the viscoelastic properties of complex fluids to the details of their microstructures at rest, and to elucidate the coupling between mechanical and structural properties. In that sense, some recent studies of complex fluids under shear flow have revealed striking analogies to equilibrium thermodynamics [8–11]. Thus, we have shown that both lyotropic and thermotropic lamellar phases present under shear flow stationnary states separated by dynamic phase transitions [8,9]. This has resulted in the construction of "non equilibrium diagrams" which represent the steady states (*i.e.* structures) adopted by the system under shear flow. Such diagrams can be represented in a plane defined by a thermodynamic variable which can be for instance the temperature or the membrane volume fraction and a dynamic variable, the shear rate or the stress. Depending on the nature of the dynamic conjugated variable (shear rate or stress) which has been chosen and on the nature of the transition, these diagrams may or may not exhibit some coexistence domains between different steady states [8,9,12].

One of the most striking feature of lyotropic lamellar phases under shear flow, is the existence of a closed compact assembly of monodisperse multilamellar vesicles (onions or spherulites) at intermediate shear rates [13,14]. Under certain conditions, this assembly may even exhibit a long range order corresponding to the crystallisation of the so-called spherulite structure [15,16]. The size of the vesicles depends on the applied shear rate, decreasing from a few microns to a tenth of a micron, as the applied shear rate increases. Although the effect of shear on lyotropic lamellar phases has received theoretical attention over recent years [17–19], the actual mechanisms leading to onion formation are still under significant debate [8] as a result of a lack of formalisms to describe strong coupling between flow and structure in complex fluids. Also, if the stationary states have been widely studied [13,20,21], very little is known about the transient behaviour. In order to elucidate this question, we have recently started to investigate the dynamics of formation of onions using different technics under shear flow such as small angle light scattering, direct observation under microscope and conductivity measurements. To begin, we have focused on how the onions change size when the control parameter is the shear rate.

Diat [8] has observed that the onion size depends on shear rate. In the stationnary state, the dynamics of size change in onions can therefore be probed merely by

[a] *Present address*: Centre de Physique Moléculaire Optique et Hertzienne, Université Bordeaux-I, 351 cours de la Libération, 33405 Talence, France.
e-mail: ppanizza@iris.cpmoh.u-bordeaux.fr

changing the shear rate. The onion size varies as the inverse of the square root of shear rate [8]. Indeed, this relation is so far not understood. A first model proposed by one of us, based on a balance between the viscous and the elastic stress stored in the onion, explains the experimental relation observed between size and shear rate [22]. Nevertheless, this model misses the size dependence on dilution (*i.e.* on membrane volume fraction) at a given shear rate. The experiment shows a $\Phi^2$ dependence while this model prediction leads to a $\Phi^{1/2}$ dependence. Another model by Bergenholtz [23] assumes instead that the onion size results from a balance between the viscous stress and the stress required to deform the onion [21,24]. If the viscosity varies as the inverse square root of the applied shear rate and not with dilution, this model leads for the onion size to the correct scaling with shear rate and dilution. However it is well established for the system we study here that the onion steady state viscosity does not satisfy this condition [10]. A complete understanding requires clearly more experimental and theoretical investigations. We expect experimental studies of transient behaviour to help in providing information about the physical mechanism fixing the onion size.

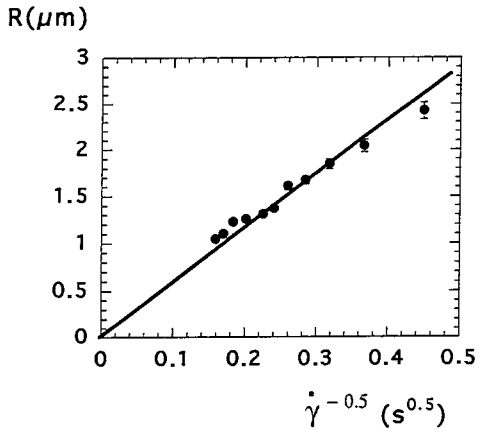


**Fig. 1.** Variation of the onion size with the applied shear rate. The size is measured using the position $q_{max}$ of the peak obtained in small angle light scattering by the relation: $\Re = \pi/q_{max}$. The system is a lamellar phase consisting in mass fraction of 15.75% SDS, 14.8% pentanol, 24.45% water and 45% dodecane. The size varies as the inverse of the square root of shear rate. The best fit (full line) gives: $\Re\,(\mu\text{m}) = 5.8/\sqrt{\dot{\gamma}}\,(\text{s}^{-1})$.

## 2 Experiments

### 2.1 Material

The system we studied is a quarterny mixture of sodium dodecyl sulfate (SDS), water, pentanol and dodecane. The phase diagram of this system has been widely studied for a water over surfactant mass ratio of 1.55 [25,26]. For this ratio, it shows a very large lamellar domain stabilized by undulation interactions [27]. Upon dilution, which consists of adding dodecane+pentanol (9% in weight) to a concentrated lamellar phase, it is possible to vary the repeating distance from 4 to 40 nanometers [26,28]. The orientation diagram of this system has also been also very well studied [8]. At low and high shear rates, the lamellae are mainly oriented perpendicular to the shear gradient direction. For intermediate shear rates, there exists a state made of closed compact and monodisperse multilamellar vesicules (so called "onions"). The onion radius $\Re$ varies as the inverse of the square root of the shear rate (Fig. 1) in agreement with results reported by Diat *et al.* [8]. We studied a lamellar consisting in mass fraction of 45% dodecane, 15.76% SDS, 14.8% pentanol and 24.44% water, for which the repeating distance $d$ is 8 nanometers. For this composition, the onion state is stable over a wide range of shear rates (between 1 and 800 $\text{s}^{-1}$).

### 2.2 Shear cells

#### 2.2.1 Small angle light scattering

A Couette cell made of plexiglas cylinders was used for small angle light scattering (Fig. 2). It consists of two concentric cylinders whose radii are 24 and 25 mm. The

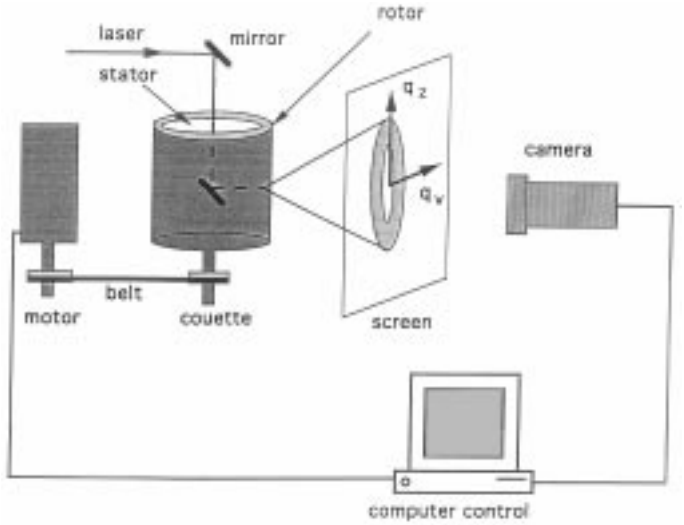


**Fig. 2.** Schematic representation of the Couette cell used for small angle light scattering measurements.

inner cylinder (stator) is kept fixed while the outer one (rotor) rotates. Simple Newtonian fluids exhibit with such flow geometry quasi-constant shear rate. However, when the gap is filled with non-Newtonian materials (such as liquid crystals for instance), the flow becomes more complex. Nevertheless, we keep the name shear rate and notation $\dot{\gamma}$ for the quantity $\rho\omega/e$ (where $\rho$, $\omega$ and $e$ represent respectively the rotor radius and its angular velocity, and the gap). Indeed, this quantity represents the mean shear rate through the gap. Depending upon rotor angular velocity, the shear rate varies from 0 to 2000 $\text{s}^{-1}$. This cell is thermostated and the temperature is controlled within 0.5 K. The light source is a 30 mW He-Ne laser. The incident beam is parallel to the shear gradient direction and

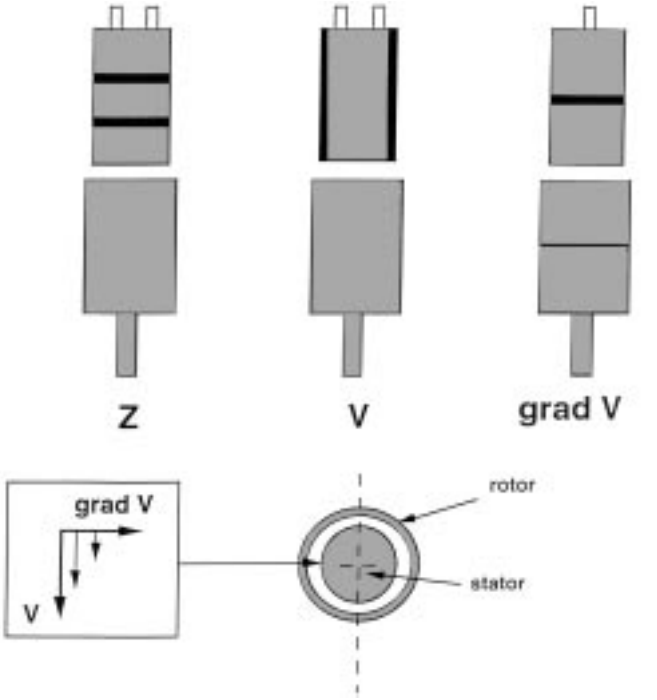


**Fig. 3.** Schematic representation of the Couette cells used for electrical conductivity measurements. Three sets of cells allow the measuring of the conductivity in the three main directions of the shear flow. For each geometry, electrodes (represented in black) are mounted on symmetry grounds.

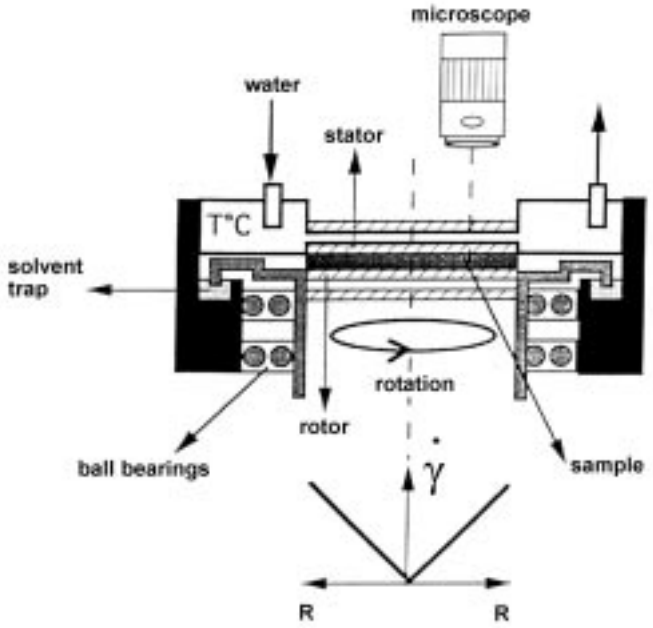


**Fig. 4.** Schematic representation of the plate to plate cell used for microscopic observations. The shear rate varies linearly with distance to the rotation axis.

then probes scattering in the plane $q_V$ (parallel to the fluid velocity) and $q_Z$ (parallel to $Z$, the vortex direction). The diffusion pattern is visualized on a screen at distance $D$ from the scattering volume. Images are recorded as a function of time with a visual acquisition card (I2S, Pessac, France). Numerical treatments such as Isotropic and Angular can then be performed.

### 2.2.2 Shear cells for conductivity measurements

Conductivity measurements under shear flow have been performed on Couette cells whose radii are 27 and 28 mm (Fig. 3). Both the stator and rotor are made of insulating material and equipped with electrodes. In order to access the conductivity in the three main directions ($V$, Grad $V$, $Z$), three different sets exist. The position of the electrodes is determined for each set on symmetry grounds. The electrodes are connected to a Lock-In Amplifier which allows measurement of the complex impedance in the large frequency range (1 Hz to 15 MHz). The impedance measured by the Lock-In can then be related to that of the sample once corrections for polarisation effects and connections are determined [29]. Conductivity and Dielectric constants at frequency $f$ can be derived from the complex admittance $Y$ of the sample measured:

$$Y = \lambda_r \sigma + 2\pi f \varepsilon_0 \varepsilon_r \lambda_c,$$

$\lambda_r$ and $\lambda_c$ are cell constants that have been determined measuring a series of salted water and pure alcohol solutions whose conductivity and dielectric constants are known. The conductivity of the lamellar phase we studied has no frequency dependence in the range 1 kHz-100 MHz whatever the shear rate and direction are. All our measurements were made at 10 kHz. Since no frequency dependence is found, the results at this frequency can be identified to the conductivity at zero frequency. A home made program allows us to monitor the shear rate and to record the time evolution of the conductivity.

### 2.2.3 Visual observations

Observations in direct space have been performed under optical microscope between crossed polarizers. The shearing cell is a plate/plate cell [8] that can fit in the microscope (Fig. 4). Such a cell consists of two parallel circular glass plates 1 mm apart from each other. One of the plate rotates while the other is kept fixed. The shear rate is no longer constant in the cell but varies linearly with the distance from the rotation axis. The cell is sealed to avoid evaporation and thermostated within 0.5 °C.

## 3 Results

In the stationnary state, the onion radius $\Re$ varies as the inverse of the square root of the shear rate (Fig. 1). It is therefore possible by increasing (decreasing) the shear rate to decrease (increase) the onion size. In order to investigate the transient behaviour of such processes, we have adopted the following procedure. First, we apply a shear rate for a long time (a few hours) in order to prepare initial

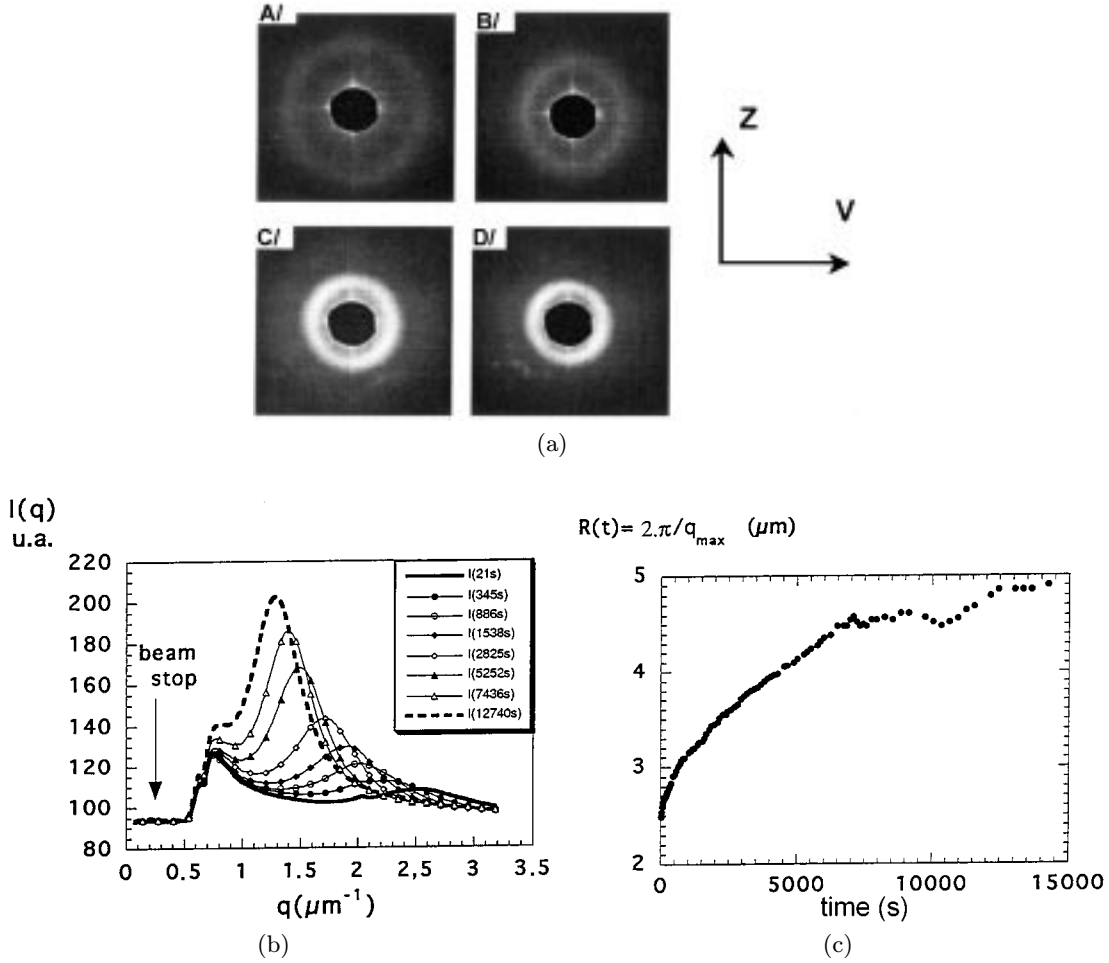


**Fig. 5.** (a) Evolution of the small angle light scattering pattern following a decrease in shear rate from 25 to 5 $s^{-1}$. The figure of scattering is vizualized on a screen. Photograph A represents the figure of scattering of the initial onions prepared at 25 $s^{-1}$. Photographs B, C and D are respectively taken 345, 2825 and 1270 seconds after changing the shear rate. (b) Time evolution of the isotropic profiles corresponding to Figure (a). (c) Time evolution of the characteristic size $R$ giving rise to the Bragg ring: $R(\mu\text{m}) = 2\pi/q_{max}$. The steady state is obtained after four hours approximately.

onions in their stationnary state. Once the steady state is obtained, we change suddenly the value of the shear rate. As a result, the system is no longer in equilibrium, and evolves to its new steady state. Using light scattering, visual observation and conductivity measurements, we follow the evolution of the structure as a function of time.

By small angle light scattering, two different mechanisms (continuous and discontinuous) can be distinguished for each process (increasing and decreasing the onion size). We name continuous (respectively discontinuous) transient regimes where the Bragg peak moves continuously from its initial to its final position (Figs. 5 and 6) or not (Figs. 7 and 8). For discontinuous regimes, first the contrast of the initial Bragg peak decreases , then a new Bragg peak appears directly at its final position (Fig. 8). A dynamic diagram which represents the nature (continuous or discontinuous) of the observed regime as a function of initial and final shear rate is depicted in Figure 9. In this figure, one can note that for a given initial shear rate, continuous transient regimes occur when the amplitude of change in shear rate $\Delta\dot{\gamma} = |\dot{\gamma}_{initial} - \dot{\gamma}_{final}|$ is small enough. From now on, we limit our presentation to experiments where the onion size increases.

Under the microscope, the onion texture in its steady state shows clearly the micrometer modulation of the refractive index which gives rise to the ring observed in light scattering. For continuous regimes, the characteristic length scale of this index modulation increases continuously in agreement with the continuous displacement of the Bragg ring observed in light scattering (Fig. 10a). This evolution of the texture is homogeneous within the cell. For discontinuous regimes, the evolution of the texture is different (Fig. 10b): it involves two stages. First, the initial texture transforms slowly to that of a lamellar phase with some defects. The micrometer modulation of the index vanishes in the whole cell volume. The onions break and free the membrane that orientates with some defects in the flow direction. In the second stage, a new modulation

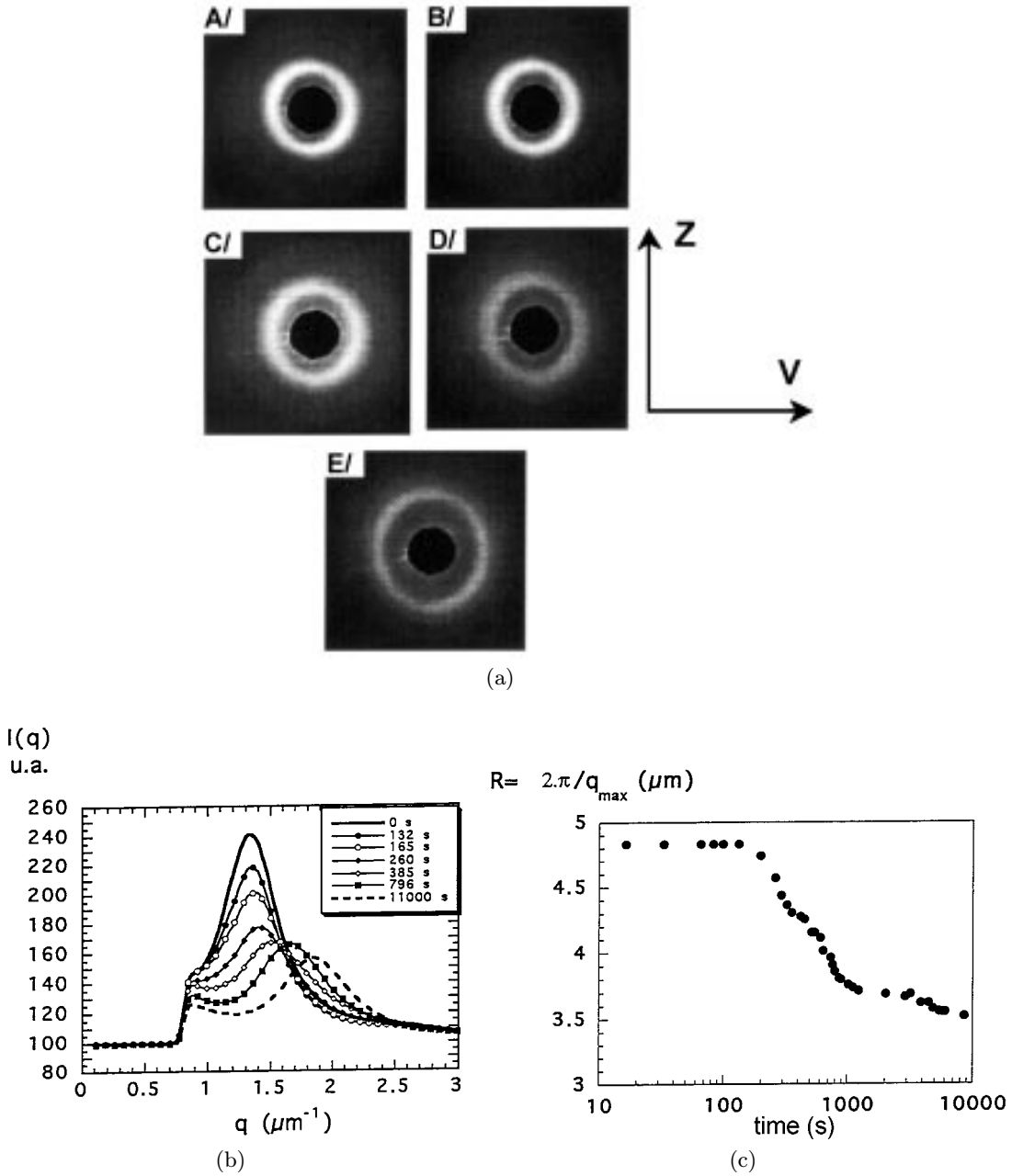


**Fig. 6.** (a) Evolution of the small angle light scattering pattern following an increase in shear rate from 5 to 10 $s^{-1}$. Photograph A represents the initial scattering pattern at 5 $s^{-1}$. Photographs B, C, D and E are respectively taken at 132, 260, 796 and, 11000 seconds after changing the value of shear rate to 10 $s^{-1}$. (b) Time evolution of the isotropic profiles corresponding to Figure (a). (c) Time evolution of characteristic size $R$ giving rise to the Bragg ring.

of the index appears. The contrast of this new modulation increases while its characteristic length scale stays. This latter stage is revealed in light scattering through the emergence of the Bragg peak directly at its final position (Fig. 7). This suggests either a nucleation process or a spatial hydrodynamic instability mechanism. So far, from observations in direct space, we have not been able to draw a definite conclusion. It is indeed very difficult looking at Figure 10b to decide whether the new index modulation appears homogeneously within the cell volume (hydrodynamic instability [30]) or inhomogeneously (nucleation [31]). In light scattering, the first stage corresponds to a decrease of the intensity of the initial Bragg ring. Such an intensity decrease is not visible in Figure 7 (The initial ring is out of the scope of the screen). We have indeed never been able to observe it because of the optical limitation of our set-up. Situations where the initial bragg ring is visible ($\dot{\gamma} < 50$ $s^{-1}$) lead always, when we decrease

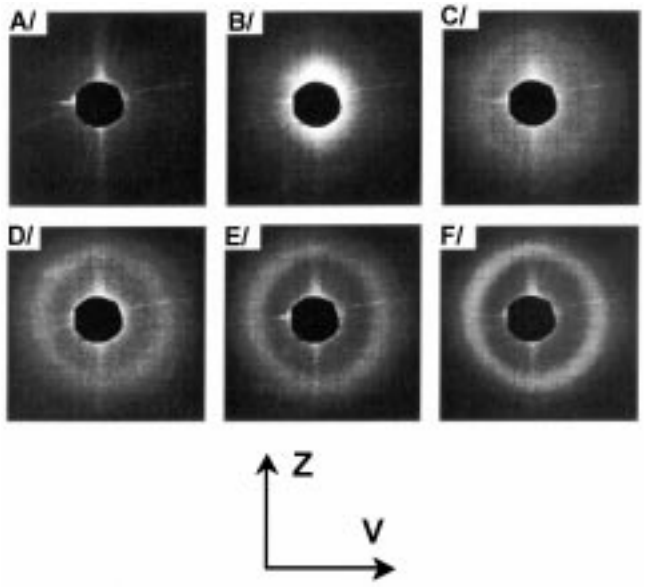


(a)

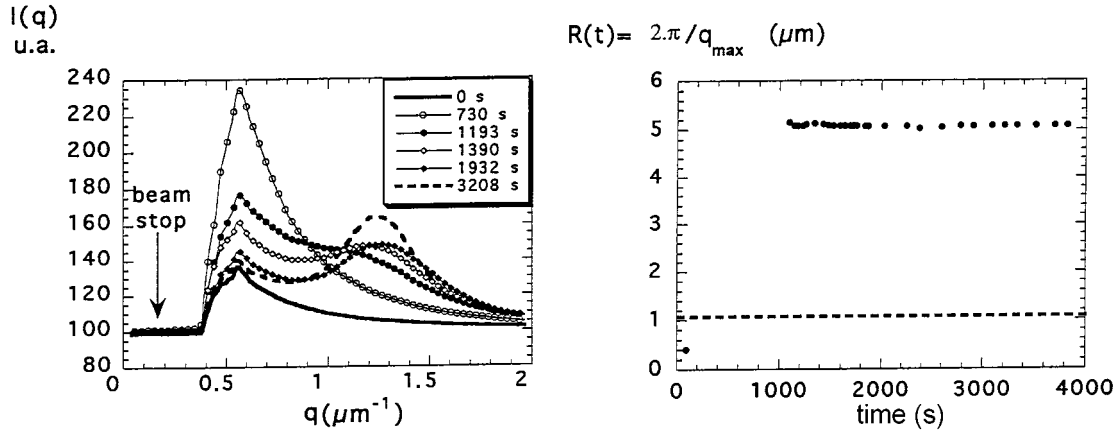


(b) (c)

**Fig. 7.** (a) Evolution of the small angle light scattering pattern following a decrease in shear rate from 200 to 5 $s^{-1}$. Photograph A represents the initial scattering pattern at 200 $s^{-1}$. Photographs B, C, D, E and F are respectively taken after 730, 1193, 1390, 1932 and 3208 seconds after changing the value of shear rate to 5 $s^{-1}$. (b) Time evolution of isotropic profiles corresponding to Figure (a). (c) Time evolution of the characteristic size $R$ giving rise to the observed Bragg ring. It is not possible with our set up to determine characteristic size below 1 micron. The dashed line represents this optical limitation. So, in order to measure the size of onions prepared at 200 $s^{-1}$, we removed the initial texture from the Couette cell and placed it in a test tube to perform a measurement of the intensity scattered at large angles. Remember that the onions are metastable once the shear flow is stopped.

the shear rate (*i.e.* increase the onion size), to continous regimes (see Fig. 9). However, such an intensity decrease can be seen when we increase the shear rate (*i.e.* decrease the onion size) (Fig. 8b).

We have determined the characteristic times associated with both mechanisms by conductivity measurements in the three main directions ($V$, grad $V$, $Z$). For both regimes, we have checked that the characteristic times we deduced from conductivity data (see below) are independent of the direction of measurement. Therefore, we will present here only results obtained in the $Z$ direction.

For continuous regimes, the transient conductivity can be empirically well fitted by the sum of two exponentials (as shown in Fig. 11a). The two characteristic times always differ sufficiently, approximatly by an order of magnitude, to believe in their physical significance despite the absence of a real physical model to parameterize the data. The longest time which varies from a few hundreds to a few thousands of seconds, corresponds in light scattering experiments to the continuous displacement of the Bragg ring. The shortest time (which varies from a few tens to a few hundreds of seconds), seems to correspond in small

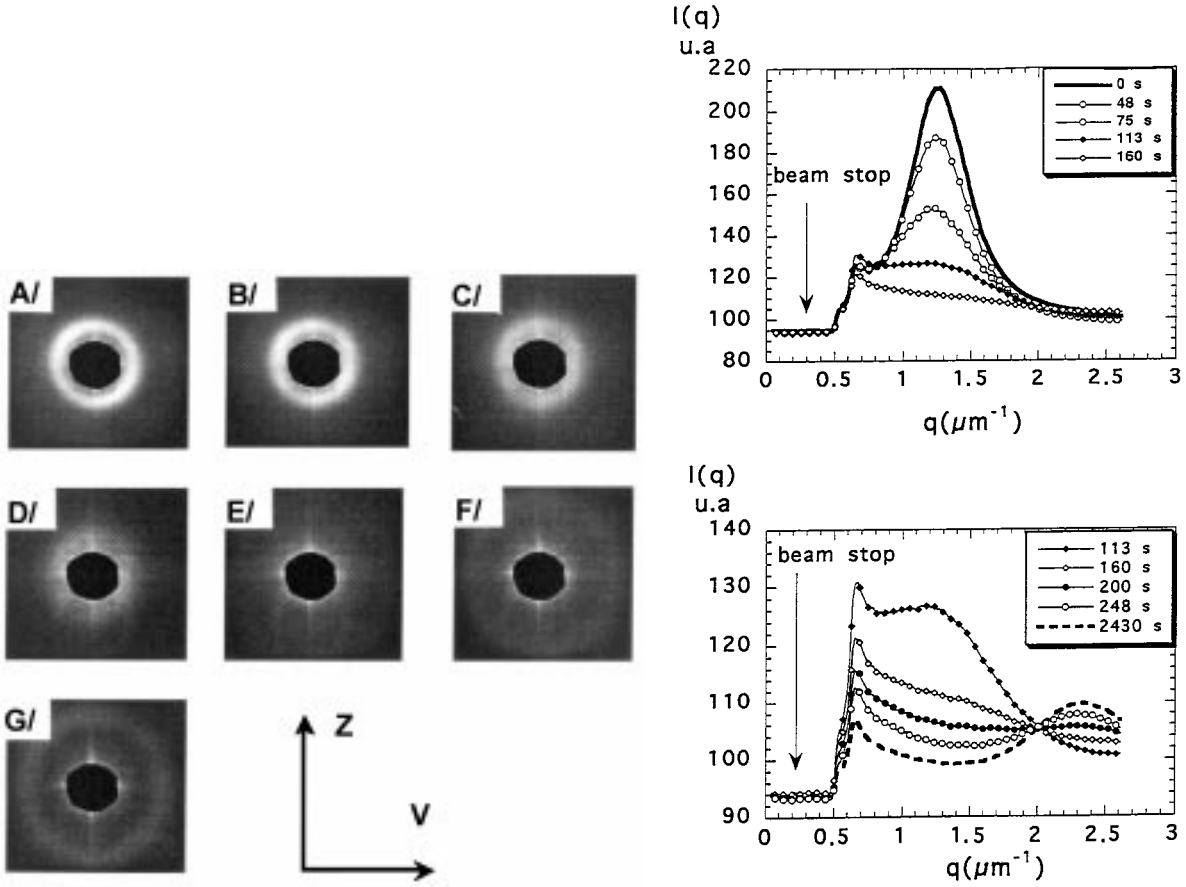


(a) (b)

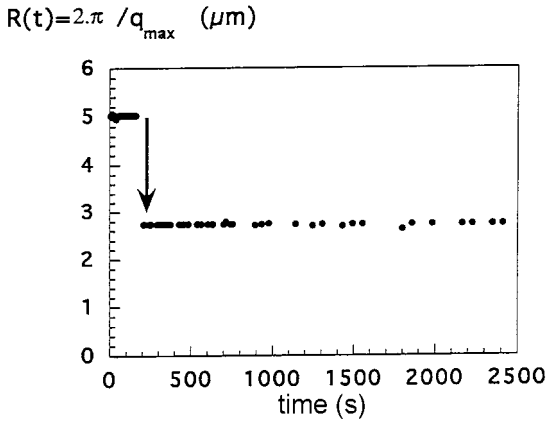


(c)

**Fig. 8.** (a) Evolution of the small angle light scattering pattern following an increase in shear rate from 5 to 25 $s^{-1}$. Photograph A represents the initial diffusion pattern at 5 $s^{-1}$. Photographs B, C, D, E, F and G are respectively taken after 48, 75, 160, 1932 and 3208 seconds after changing the value of shear rate to 25 $s^{-1}$. (b) Time evolution of the isotropic profiles corresponding to Figure (a). (c) Time evolution of the characteristic size $R$ giving rise to the Bragg ring.

angle light scattering measurements, to a decrease of the contrast of the initial Bragg ring (Figs. 6a and b). We have precisely checked that both of the charateristic times depend on the final shear rate (*i.e.* final onion size) but not of the initial one (*i.e.* initial onion size). They decrease rapidly with the final shear rate. Morever, their values do not depend on whether the shear rate is increased or decreased provided that the value of the final shear rate is the same and that the transient regimes observed upon increasing and decreasing the shear rate are both continuous. The longest time decreases exponentially with the final shear rate (Fig. 12).

For the discontinuous regimes, transient conductivities cannot any longer be fitted by two exponential relaxations. The conductivity signal is more complex (Fig. 11b). It shows a bump probably related to the orientation of the membranes freed by the breaking of the initial onions. However, the conductivity seems still to vary exponentially at long times. The characteristic time associated to that exponential relaxation, is of the order of several hundreds of seconds. It corresponds to the increase of the intensity of the final Bragg ring that we observe in light scattering. This time is independent of the initial shear rate (*i.e.* initial onion size). In the absence of a model to parameterize the complex conductivity signals at short times, we have not been able to determine the charateristic time associated with the first stage of discontinuous regimes (*i.e.* breaking of initial onions).

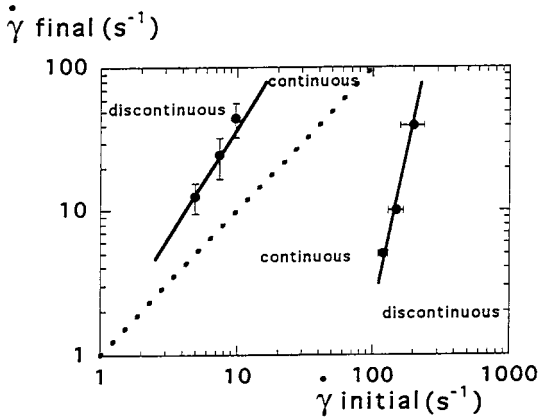


**Fig. 9.** The dynamic phase diagram gives the nature (continuous or discontinuous) of the transient regime as a function of initial and final shear rates. The dashed line corresponds to $\dot{\gamma}_{initial} = \dot{\gamma}_{final}$.

## 4 Discussion

The experimental situation is as follows. When the change of shear rates remains limited (below a critical value given in the dynamic diagram Fig. 9) the onions change continuously their size as a function of time. The kinetics can be successfully described with two characteristic times, both depending only on the final shear rate. The longest time, which can be precisely measured, is an exponential function of the final shear rate. For any given initial shear rate, above a well defined value for the difference of shear rates (see Fig. 9) the process is significantly different with a more complex behavior, involving a discontinuous change in size.

Let us first examine the continuous process. Light scattering and microscopic observations clearly indicate that the onion size change continuously. This means that the number of layers involved in each multilamellar vesicles changes continuously. The question is: how this happens at a microscopic level? A suggestion from Leibler and Prost [22] was that depending on the permeation velocity the onions can either change their size (let's say decrease) by peeling when permeation is very slow or by diffusion of matter through the layers when permeation is fast enough. Indeed, it is easy to show that taking into account the nature of the elastic energy of a spherical droplet of a smectic phase, an onion under stress sees a divergence of the stress as a function of the distance $r$ to its center as $1/r$. This indicates that the maximum of stress is supported by the last layer at the center. Upon such an increase of stress due to the change of shear rate (either negative or positive depending upon the sign of the change in shear rate) and if permeation is possible, the onion can react as follows. Since the maximum of stress is at the center there is a gradient of stress from the center to the outside, it is then possible to relax this excess of stress for a lyotropic system by permeation of matter from the center to the outside. One can imagine that the two times that we have measured correspond first to a loss of solvent diffusing quickly at fixed number of layers, then by a slow permeation process changing the number of layers. In that case, the long time would be directly related to the permeation time. Since there is no independent measurements of the permeation time, it is difficult to have a more quantitative analysis.

When the change in shear rate is large enough (*i.e.* discontinous regimes) a rather different process has been observed. From the microscopic observation, it seems that the onions are completely destroyed and a rather homogeneous texture is transiently observed (corresponding either to state I or state III). Then, an instability is generated under shear leading directly to the new size. The characteristic time is then not a function of either the final shear rate or the initial one. It is obviously very difficult to built up a realistic scenario because it clearly involves nonlinear effects. However, we are currently studying the kinetics of building the onions from either state I or state III, to see whether there are some similarities with the second part of the scenario.

## 5 Conclusion

We have investigated the dynamics of onion size changes under shear flow by means of small angle light scattering, conductivity and direct observations. We have observed two regimes: continuous and discontinuous.The nature of the regime is fixed by the initial and final values of the shear rate. For continuous regimes (*i.e.* for small enough variations of the shear rate), the characteristic length of

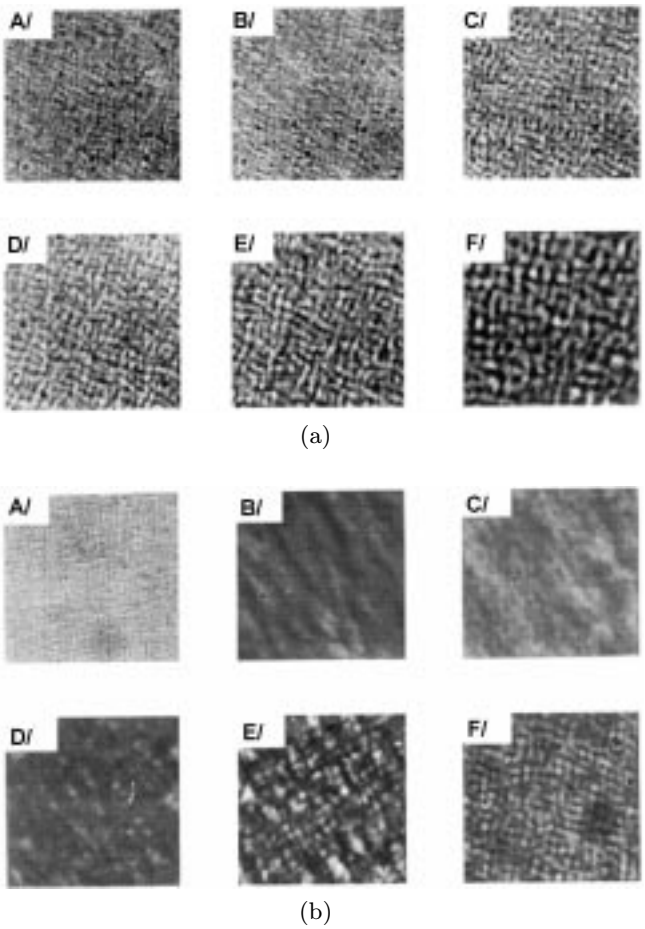


**Fig. 10.** Evolution of the texture observed under microscope between crossed polarizers following a decrease of the applied shear rate. The change of shear rate fixes the time origin. (a) Continuous regime. The shear rate decreases from 25 to 5 $s^{-1}$. Figure A represents the initial texture. Figures B, C, D, E, and F are taken respectively after 8, 24, 44, 52 and 200 minutes. (b) Discontinuous regime. The shear rate changes from 200 to 5 $s^{-1}$. Photograph A represents the initial texture. Figures B, C, D, E and F are taken respectively after 8, 20, 37, 52 and 200 minutes.

the texture (*i.e.* the refractive index modulation length scale) evolves continuously and homogeneously within the cell, similar to spinodal decomposition. The charateristic time associated with the evolution decreases exponentially with the value of final shear rate and is independent of the initial shear rate. For discontinuous regimes (*i.e.* large variations in the applied shear rate), the onions break and free the membranes that orientate along the direction of the flow. An hydrodynamic instability or a nucleation process takes place leading directly to the final onion size. The characteristic time associated with that process is independent of initial and final shear rate values.

The authors would like to acknowlege fruitful discussions with A. Arnéodo, M.E. Cates, S. Köenig, F. Nallet, F. Lequeux, P. Sierro and L. Soubiran.

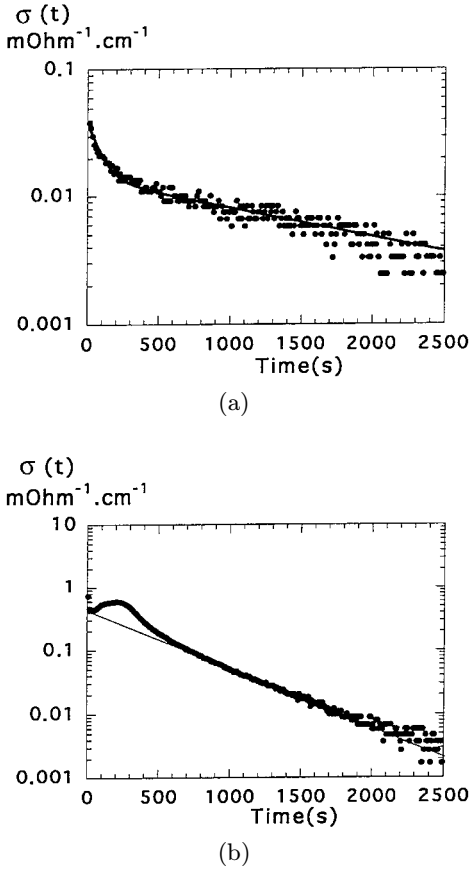


**Fig. 11.** Evolution of the electrical conductivity following a decrease of the applied shear rate. The conductivity is measured along the vortex direction. The change of shear rate fixes the time origin. (a) Continuous regime: The shear rate decreases from 25 to 5 $s^{-1}$. The signal can be well fitted by the sum of two exponential relaxations. The best fit (continous line) gives for the value of the two characteristic times 250 and 1900 seconds. (b) Discontinous regime. The shear rate decreases from 200 to 5 $s^{-1}$. At long times, the signal varies exponentialy. The best fit (continous line) leads to a characteristic time value of 400 seconds.

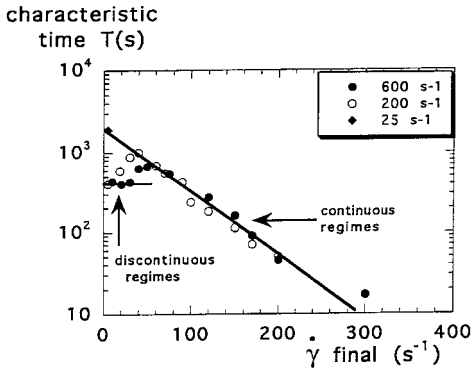


**Fig. 12.** Evolution of the longer characteristic time as a function of final shear rate. The value is determined by conductivity measurement. The value of initial shear rate is fixed to 600 $s^{-1}$ (black circles), 200 $s^{-1}$ (white circles) and 25 $s^{-1}$ (black triangles). Note that in the continuous regime, the characteristic time is independant of initial shear rate.

## References


1. see for instance: G.K. Batchelor, *An introduction to Fluid Dynamics* (Cambridge University Press, 1970).
2. N.A. Spenley, M.E. Cates, T.C.B. McLeish, Phys. Rev. Lett. **71**, 939 (1993).
3. R. Wessel, R.C. Ball, Phys. Rev. A **46**, 3008 (1992).
4. B.J. Ackerson, N. Clark, Phys. Rev. A **30**, 906 (1984).
5. C.R. Safinya, E.B. Sirota, R.J. Plano, Phys. Rev. Lett. **66**, 1986 (1991).
6. J. Yamamoto, H. Tanaka, Phys. Rev. Lett. **77**, 4390 (1996).
7. V. Schmitt, F. Lequeux, A. Pousse, D. Roux, Langmuir **10**, 955 (1994).
8. O. Diat, D. Roux, F. Nallet, J. Phys. II France **3**, 1427 (1993).
9. P. Panizza, P. Archambault, D. Roux, J. Phys. II France **5**, 303 (1995).
10. D. Roux, F. Nallet, O. Diat, Europhys. Lett. **24**, 53 (1993).
11. J.F. Berret, D.C. Roux, G. Porte, P. Lindner, Europhys. Lett. **25**, 521 (1994).
12. R. Makhloufi, J.P. Decruppe, A. Ait-Ali, R. Cressely, Europhys. Lett. **32**, 235 (1995).
13. O. Diat, *Effet du cisaillement sur les phases lyotropes: phases lamellaires et phase éponges*, Thesis, University Bordeaux-I, France (1993).
14. O. Diat, D. Roux, J. Phys. II France **3**, 9 (1993).
15. O. Diat, D. Roux, F. Nallet, Phys. Rev. E **51**, 3296 (1995).
16. P. Sierro, D. Roux, Phys. Rev. Lett. (1997).
17. P. Ostwald, S.I. Ben-Abraham, J. Phys. France **43**, 1193 (1982).
18. R. Bruinsma, Y. Rabin, Phys. Rev. A **45**, 994 (1992).
19. M. Goulian, S.T. Milner, Phys. Rev. Lett. **74**, 1775 (1995).
20. P. Panizza, V. Vuillaume, C.Y. Lu, M.E. Cates, D. Roux, Langmuir **12**, 248 (1996).
21. L. Soubiran, P. Sierro, C. Coulon, D. Roux, to be published.
22. J. Prost, S. Leibler, D. Roux, to be published.
23. J. Bergenholtz, N.J. Wagner, Langmuir, **12**, 3122 (1996).
24. E. Van der linden, J.H. Droge, Physica A **193**, 439 (1993).
25. D. Roux, A.M. Bellocq, in *Physics of Amphiphiles*, edited by V. Degiorgio, M. Corti (Amsterdam, North Holland, 1985).
26. D. Roux, Thése d'État, Université de Bordeaux-I (1984).
27. W. Helfrich, Z. Naturforsch. **33a**, 305 (1978).
28. C.R. Safinya, D. Roux, G.S. Smith, S.K. Sinha, P. Dimon, N.A. Clark, A.M. Bellocq, Phys. Rev. Lett. **57**, 2718 (1986).
29. L. Soubiran, P. Sierro, C. Coulon, D. Roux, Europhys. Lett. **31**, 243 (1995).
30. P. Manneville, *Dissipative structures and weak turbulence* (Academic Press, New-York, 1990).
31. see for instance: J.D. Gunton, M. San Miguel, P.S. Sahni, *The dynamics of first order phase transitions*, in *Phase Transitions and Critical Phenomena*, Vol. **8** (Domb and Lebowitz Eds, Academic Press, 1983).